

Serial Pushing Model for the Self-Assembly in Dip-Pen Nanolithography[†]

Hyojeong Kim and Joonkyung Jang*

Department of Nanomaterials Engineering, Pusan National University, Miryang 627-706, Republic of Korea

Received: December 12, 2008; Revised Manuscript Received: January 14, 2009

Based on the findings of molecular dynamics simulations, we propose a novel diffusion model for the self-assembly in dip-pen nanolithography. A central question in such modeling is how a nascent droplet created below an AFM tip spreads out to form a self-assembled monolayer (SAM) on a substrate later. In the present model, a molecule dropping from the tip pushes a molecule on the substrate out of its original position, and the molecule pushed out in turn pushes its own neighbor. A SAM grows through such a series of push-induced movements. The initial pushing propagates all the way to the periphery where there is no molecule to push out. By contrast, according to the previous hopping-down model, a molecule moves by stepping over molecules trapped on the substrate and occasionally hops down to the substrate. By implementing our model in random walk simulations, we study the structure and growth dynamics of the SAM generated by a fixed tip and the lines and characters created by a moving tip. We investigate how the SAM is influenced by the molecular dripping rate and tip scan speed. Compared to the hopping model, the present model gives a SAM growing faster and more fluctuating in its periphery. A salient feature of our model is its ability to generate various SAMs by changing the directional coherence length of the push-induced displacement. If we choose the coherence length to be zero, each push-induced displacement is random in direction to give a compact circular SAM. As the directional coherence length increases, the SAM becomes a noncircular pattern with distinct branches. In the limit of an infinite coherence length, the SAM becomes a long narrow cross due to the substrate anisotropy.

I. Introduction

Tip-based dip-pen nanolithography (DPN) is a powerful method to construct two-dimensional nanostructures on various substrates.^{1–3} Using a sharp AFM tip coated with molecules, DPN transfers molecules from the tip to a substrate, making a self-assembled monolayer (SAM) with a nanometer resolution. DPN succeeded in patterning various molecular types (organic molecules, polymers, DNA, proteins, peptides, and nanoparticles) on metallic, insulating, and semiconducting substrates. Numerous technological innovations of DPN have been made since its invention. For example, a microfluidic channel has been integrated into the AFM cantilevers (so-called nanofountain pen)^{4,5} to facilitate the continuous supply of molecules. Recently DPN has been equipped with massively parallel, high-throughput, and large-area capabilities by putting together tens of thousands of tips into a two-dimensional array.¹

In spite of the widespread and successful applications in biochips, nanomaterials, and semiconductor industry, our fundamental understanding of DPN is still poor. We do not know exactly how DPN is influenced by intrinsic molecular properties (e.g., diffusivity) and by external conditions such as the tip scan speed, temperature, and humidity. Theoretical investigation has proven invaluable in this fundamental aspect of DPN.^{6–20} In principle, a fully molecular simulation of DPN is desirable, but it seems difficult at the current stage. First, experimental details of DPN necessary for simulation are largely unknown. We do not know the exact geometry of the tip and substrate. It is therefore difficult to set up unambiguously the initial condition (geometry and molecular positions) for molecular dynamics

simulation. Even if such experimental details are known, DPN is quite a complicated process to simulate. Molecules initially coated on the tip have to detach themselves from the tip (solid melting), then drop down to the substrate (possibly through a water meniscus formed between the tip and substrate), and finally self-assemble on the substrate to form a SAM. Moreover, the tip must move on the substrate to create various patterns, and the typical size of a SAM is several hundred nanometers. All these seem challenging for a molecular simulation.

Instead of describing the molecular details of DPN, we seek a simplified model which captures the key features of DPN. If such a model can reproduce experimental results, it will serve as an invaluable tool for the structure prediction of DPN. One can perform computer simulations by using the model, perhaps to check the dependency on experimental conditions such as molecular diffusivity and tip scan speed. Such simulations will serve as useful feedback to experiment in an effort to achieve an optimal control of DPN. In our thoughts, a successful model of DPN must take into account the following two aspects: the molecular flow from the tip and the self-assembly on the substrate. In doing so, the model should incorporate the properties of molecule and substrate such as molecular transport property and molecule–substrate binding strength. Several phenomenological models have been proposed so far.^{8,13,14,19,20} Unfortunately, they focused on the water meniscus formed between the tip and substrate^{14,19,20} or did not consider the case of a moving tip.^{8,13}

Based on a set of simplifying assumptions, we have proposed a hopping down model for DPN (Figure 1a) that can be applied to the case of a moving tip.⁶ Due to the molecular flow from the tip, the substrate area below the tip is congested with molecules (unlike the area far from the tip). The consequent concentration gradient drives the molecular diffusion away from

[†] Part of the “George C. Schatz Festschrift”.

* Corresponding author. E-mail: jkjang@pusan.ac.kr. Fax: +82-55-350-5653.

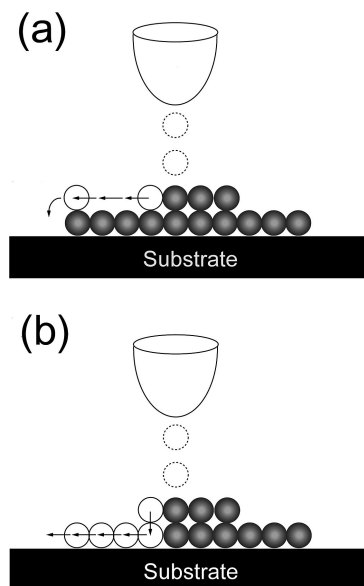


Figure 1. Two models of the self-assembly in dip-pen nanolithography. When an AFM tip is put into contact with a substrate, molecules (dotted circles) start to drop from the tip to the substrate, forming a multilayered droplet. (a) Hopping down model. A molecule on top (open circle) steps over the immobile molecules touching the substrate (gray circles at the bottom). Once a molecule reaches the edge of the monolayer of immobile molecules, it hops down to the bare substrate and gets trapped. (b) Serial pushing model. A molecule on top of the bottom layer (open circle in the second layer) pushes its way down to the bare substrate. To do so, molecules at the bottom have to move toward the periphery to make a room for the pushing down molecule. In the figure, four molecules (drawn as open circles in the bottom layer) move collectively toward the periphery.

the tip toward the unoccupied area of the substrate. Central to the model is the mechanism of how a nascent droplet spreads out to form a SAM afterward. If we assume an extremely strong molecule–substrate binding, molecules become trapped once they touch the bare substrate, forming a monolayer at the bottom (drawn as gray circles at the bottom in Figure 1a). Molecules deposited earlier in time soon cover up the area under the tip. Molecules dropped later, since the area near the tip is preoccupied, step over molecules below and occasionally hop down to the bare substrate (once they reach the SAM periphery). This hopping model should be valid in the limit where the molecule makes an irreversible, extremely strong (usually chemical) binding to the substrate.

Recently, we performed molecular dynamics (MD) simulations^{9,10} for an alkanethiol on gold (111) substrate, a prototypical system for DPN. Instead of the irreversible trapping of molecules as in the hopping model, molecules rearrange on the substrate through a serial pushing mechanism (Figure 1b). More specifically, a molecule in the upper layer (open circle in the second layer in the figure) pushes a molecule on the substrate out of its original position, and the molecule pushed out in turn pushes out another molecule nearby. The underlying reason is that, although thiol molecules strongly stick to the gold, they can move rather easily from one of hollow sites of Au (111) to another. Their vertical movements on the substrate are severely restricted, but their lateral movements are relatively facile (like a magnet on a magnetic board). If such a successive push propagates and hits the periphery, the pushing finally stops and the SAM grows in size. The serial pushing prevails for a SAM with a diameter up to 40 nm. For such a large monolayer, the serial pushing involves a concerted displacement of many molecules to reach the periphery. Herein, adopting the above pushing mechanism,

we develop a novel diffusion model and implement it in random walk simulations. We inspect SAMs created by using various molecular dripping rates, ns , and scan speeds, vs , of the tip. For a tip fixed or moving on the substrate, we examine the growth dynamics and the shape of the SAM. We discuss qualitative and quantitative difference between SAMs obtained from the pushing and the hopping models. We show that, by changing the degree of directional coherence in the push-induced displacement, the present model can generate various structures ranging from a compact dot to a noncircular pattern with distinct branches.

II. Details of Model and Simulation

We describe how we model the molecule–substrate interaction. A molecule on the bare substrate is not allowed to move spontaneously but is displaced by push from its neighbor molecule (vertically above or laterally beside the molecule). We found that the spontaneous molecular movement on the bare substrate is insignificant in the MD simulation of alkanethiol on gold. If we allow the spontaneous molecular diffusion on the substrate, the resulting SAM will eventually diffuse away. Such a problem of no permanent SAM might be fixed by introducing intermolecular attraction to our model. In doing so, we are likely to add another parameter to our model. Instead of an elaborate model requiring more parameters, we here develop a simplistic model which, with a minimal number of parameters, can capture the essential features of DPN.

Our random walk simulation is conducted with a discrete time step dt on a cubic grid with spacing l . In all the results presented here, length and time are in units of l and dt , respectively. At every time step of simulation, each molecule sequentially executes a random walk (as opposed to the case where all the molecules move simultaneously). We randomly choose the order of sequence in which each molecule moves. Each molecule jumps from its current position (x, y, z) to one of its five nearest neighbors, $(x \pm 1, y, z)$, $(x, y \pm 1, z)$, and $(x, y, z - 1)$, with equal probability (20%). We leave out the upward jump to $(x, y, z + 1)$ because molecules, designed to bind to the substrate, should feel downward attraction from the substrate.

We explain how to implement the serial pushing mechanism in simulation. A random jump of a molecule described above is likely to cause an overlap of the jumper with one of its nearest neighbor molecules. When this overlap happens, the neighbor molecule gives up its position and becomes the next jumper to jump to one of its own nearest neighbor positions. If another molecule preoccupies the position to which the second jumper moves, a new push-induced movement follows. Note the pushing can occur in the downward direction as well as in the lateral direction. It also takes place both in one of the upper layers and in the bottom layer (see Figure 1). If the push from the upper layer propagates downward and hits a molecule on the substrate, the push changes its direction toward one of four lateral directions on the substrate. In other words, if a molecule on the substrate is pushed down by a molecule above, it laterally jumps to one of its four nearest neighbor positions. On the other hand, if a molecule on the substrate is pushed laterally by its neighbor, its push-induced jump can take only three directions because the direction toward the position of pushing molecule should be excluded. This pushing propagates toward the periphery of SAM, and it continues until there is no more overlap of the last jumper molecule with one of its nearest neighbor molecules. We take the above push-induced movements to occur without time delay. This is reasonable because each push arises from a momentum transfer between colliding

molecules and therefore should occur much faster than diffusion (note dt is a time scale within which the velocity relaxation of the molecule is complete).

An important question in our model is in what direction a molecule should move if pushed by another molecule (except that it cannot move toward the position of the molecule pushing it). Given that the pushing arises from a collision of two molecules, it can be directed toward any direction in the continuous space. We also found in MD simulations that a molecule (alkanethiol) pushed out takes a random direction in its lateral movement on the substrate (gold).^{9,10} To emulate this uniformity in direction, each direction of a push-induced jump is taken to be equally probable. Specifically, if pushed down from above, a molecule located at $(x, y, 1)$ on the substrate ($z = 0$) jumps to one of its four nearest neighbor positions on the substrate, $(x \pm 1, y, 1)$ and $(x, y \pm 1, 1)$, with equal probability (25%). If a molecule on the substrate is pushed laterally, it laterally jumps with equal probability (33.3%) toward one of its nearest neighbor positions except the position of the pusher molecule (only three directions are possible). If a molecule in the upper layer ($z > 0$) is pushed down from above, it jumps with 20% chance to one of its five nearest neighbor positions. If a molecule in the upper layer is pushed laterally, it jumps with 25% probability to one of its nearest neighbor positions excluding the position of pushing molecule (only four directions allowed).

We can make the above push-induced movement directionally more coherent by using a finite directional coherence length, N_d . This length is defined as the number of push-induced movements with the same direction: if a molecule initially pushes out its neighbor molecule, the following $(N_d - 1)$ consecutive movements take the same direction as the initial pushing direction (except the automatic vertical to lateral direction change when a molecule on the substrate is pushed down from above). Then the direction of the $(N_d + 1)$ th molecular displacement becomes random, and the subsequent $(N_d - 1)$ movements take the same direction as the $(N_d + 1)$ th displacement. This coherent pushing goes on like this until the last pushing hits the SAM periphery and stops. Our default scheme (random direction for every jump) corresponds to the case of $N_d = 0$. In the opposite limit of $N_d = \infty$, the pushing direction remains identical all the way from its start to end. We additionally considered finite coherence lengths, $N_d = 5$ and 10, which lie between the two limits of N_d . It is shown later that, depending on N_d , the SAM drastically varies in shape, ranging from a compact dot to a highly branched SAM.

The AFM tip produces a constant flux of molecules called dripping rate, n . The constancy of dripping rate has been reported in many experiments.^{11,13,14,16} In simulation, we are concerned with the relative value of dripping rate with respect to the diffusion time scale, $n^* = n/dt$ (n^* is the number of molecules dropped per time step). The case of $n^* < 1$ is called a slowly dripping tip, and one molecule is dropped for every $1/n^*$ time steps (n^* is chosen to give an integer value of $1/n^*$). The area of molecular dropping is limited within a square of nine grid points. The precise lateral position to drop a molecule is chosen at random out of nine grid points. After fixing the lateral position, we add a molecule on top of the molecule with the highest vertical position at that lateral position. In the case that there is no molecule at the lateral position, the dropping molecule is placed on top of the substrate. For $n^* = 1$, we drop one molecule at each time step by using the same procedure as for $n^* < 1$. In the case of a fast dripping tip ($n^* > 1$), n^* molecules are dropped from the tip at every time step. As above,

the lateral positions of n^* molecules lie within a square of nine grid points. If n^* exceeds 9, we put the extra $(n^* - 9)$ molecules on top of the square and their lateral positions are chosen randomly out of nine grid points of the square. Each dropping molecule is placed on top of the molecule with the highest vertical position at its lateral position or directly on the substrate (in the case that there is no molecule preoccupying the lateral position). We chose the above particular area of molecular dropping (nine grid points) to emulate a point source of molecules. With this simple choice, we focus on the self-assembly process of DPN. The previous hopping down model and the analytic diffusion theory both have been formulated by treating the tip as a point source. As long as the dropping area is small, the outcome of self-assembly will not depend much on the number of grid points for the dropping area. In real experiments, the area of molecular dropping will change from tip to tip and from time to time on a microscopic time scale. Unfortunately, not much is known about the tip geometry and the area of molecular dropping in DPN. We are currently working on a better modeling of the molecular dropping events by investigating the dropping events in molecular dynamics simulations.

In the case of a tip moving with a speed of v , the relative velocity, $v^* = v/(l/dt)$, matters in simulation. For a tip moving slowly, $v^* < 1$, the tip is displaced by one grid point for every $1/v^*$ time steps ($1/v^*$ is chosen to be an integer). If $v^* \geq 1$, the tip moves v^* grid points per time step. If the lateral position of a dropping molecule does not exactly coincide with one of the grid points on the substrate (e.g., when the tip moves diagonally or its scan speed is not commensurate with the grid), the lateral position of molecule is taken to be its nearest grid point. We constantly check in simulation whether each grid point of the substrate is stacked with molecules continuously from bottom up as in the solid-on-solid model for crystal growth.²¹ If a grid point of the substrate is not properly stacked with molecules, we adjust the vertical positions of molecules located above that grid point. For example, suppose a grid point of the substrate, $(x, y, 0)$, is initially stacked with molecules having vertical positions 1, 2, and 3: $(x, y, 1)$, $(x, y, 2)$, and $(x, y, 3)$. Let us assume the middle molecule at $(x, y, 2)$ jumps to another lateral position so that we are left with molecules located at $(x, y, 1)$ and $(x, y, 3)$. Then the vertical position of the top molecule $(x, y, 3)$ is adjusted to $(x, y, 2)$.

For comparison, we completed random walk simulations using the hopping down model. In brief, as soon as a molecule arrives at an unoccupied grid point on the substrate, it becomes immobile. A random walk is allowed only on top of the monolayer consisting of immobile molecules touching the bare substrate. If a molecule jumps to a position preoccupied by another molecule, that jump is rejected. This is in accord with the conventional excluded volume effect in random walk simulation. One can imagine that, compared to the pushing model, the molecular movement is suppressed. See ref 6 for further details.

The present work investigates the structure and growth dynamics of SAM by systematically varying the dripping rate and scan velocity of the tip, sampling the parameter space of our model. To compare with a specific experiment, we need to specify the grid spacing l and time step dt in physical units. Note l is the distance of closest approach of two molecules in simulation. For octadecanethiol on Au (111), we set $l = 0.5$ nm according to the experimental SAM structure (0.5 nm is the distance between adjacent thiol molecules of SAM).⁴ If no experimental measurement can be related to the grid spacing,

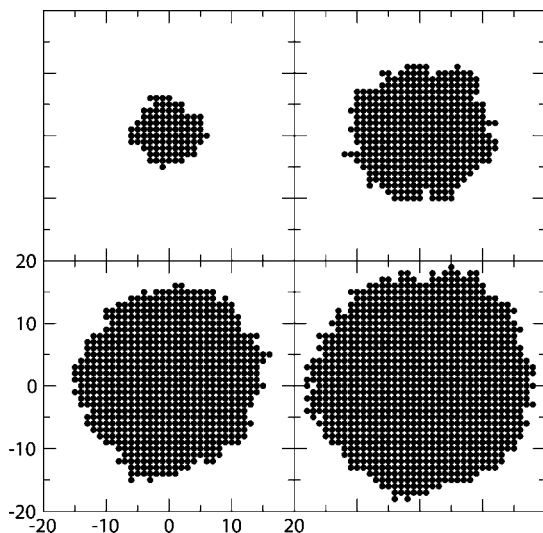


Figure 2. Growing self-assembled monolayer in the random walk simulation using the serial pushing model. Shown are snapshots taken at $t = 100$ (top left), 300 (top right), 700 (bottom left), and 1000 (bottom right). The tip is fixed in position, and its dripping rate is $n^* = 1$. In this and all the following figures, length and time are in units of the grid spacing and the time step of random walk, respectively.

we might approximate it as the effective diameter of molecule (assuming two spherical molecules in contact at their closest approach). The time step dt can be given a physical dimension as follows. If the molecular diffusivity D is known, we use the correspondence between the random walk and continuous space diffusion given by $dt = l^2/(4D)$.⁶ Notice D refers to the molecular diffusion in the upper layers, not the surface diffusion on the bare substrate. We here approximate it as the bulk self-diffusion coefficient. If the bulk diffusivity is not available, it can be estimated from viscosity η by using the Stokes–Einstein relation,²² $D = (k_B T)/6\pi\eta r$, where r is the effective radius of the molecule. For octadecanethiol on Au (111), we take η as the viscosity of octadecane at 323.15 K under atmospheric pressure ($=2.46 \times 10^{-3}$ Pa·s).²³ Using the viscosity and taking the radius r as $l/2$ ($=0.25$ nm) we get $D = 3.6 \times 10^{-6}$ cm² s⁻¹ and $dt = 176$ ps for $T = 298$ K.

III. Results and Discussion

We illustrate the growth process of SAM resulting from the serial pushing model. Figure 2 shows four consecutive snapshots for the SAM created by a tip fixed in position at the origin. With a dripping rate of $n^* = 1$, the tip is continuously dropping molecules from $t = 0$ to 1000. Snapshots are taken at $t = 100$ (top left), 300 (top right), 700 (bottom left), and 1000 (bottom right). Molecules above the bottom layer are not shown. On the whole, the SAM is isotropic and circular in shape. Due to the random nature of diffusion, however, the SAM periphery deviates from a circle, especially for the small SAMs at early times (top two panels). We quantify the deviation of the SAM periphery from a circle as follows. We first sort out the peripheral points of SAMs by defining them as molecules with less than four nearest neighbors on the substrate. We calculate the average μ_R and the standard deviation σ_R of the distances of peripheral points from the center. μ_R can be identified as the radius of a circle with the same size as the SAM. σ_R represents the deviation of the SAM from that circle. We found μ_R values of 5.1, 10.7, 14.4, and 17.3 for the top left, top right, bottom left, and bottom right of the figure, respectively. σ_R values are 0.75, 0.83, 0.89, and 0.82, respectively, for the top left, top right,

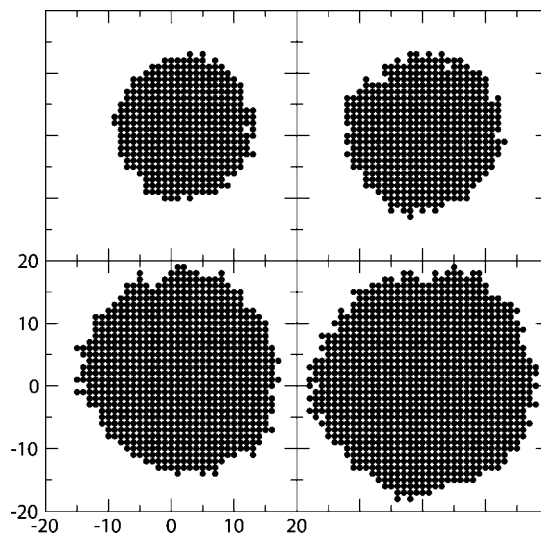


Figure 3. Comparison of monolayers obtained from the serial pushing and the hopping down models. Snapshots for the serial pushing (hopping down) model are drawn in the top right (left) and bottom right (left) panels. The tip contact times t are 500 and 1000 for the top two and the bottom two panels, respectively.

bottom left, and bottom right of the figure. As the tip contact time t increases, μ_R increases but σ_R remains about the same. We previously introduced a circularity N as an estimate of how close the SAM is to a circle.⁶ It is defined as the number of sides of an imaginary polygon that mimic the SAM periphery and is given by $N = 1.3869(\mu_R/\sigma_R)^{0.4721}$.²⁴ A large N indicates a close resemblance to a circle (N is infinity for a circle). Using μ_R and σ_R above, we found N values in Figure 2 of 3.4 (top left), 4.7 (top right), 5.2 (bottom left), and 5.9 (bottom right). These N values quantitatively show that the SAM becomes increasingly circular as it grows in size.

In Figure 3, we compare the SAMs from the pushing and the hopping models. Shown are snapshots of both the models taken at $t = 500$ (top two panels) and 1000 (bottom two panels). All the simulation conditions are identical to those in Figure 2. At a given time, the SAM from the pushing model (top right and bottom right) is larger than that from the hopping model (top left and bottom left). At $t = 500$, there is a hole near the periphery of the SAM for both models. The SAM periphery sometimes has a local geometry that looks like a rectangular trench which is two molecules deep and one molecule wide. Later, a protrusion of molecule in the periphery can accidentally close the open entrance of the trench. Holes in the figure are formed in this way. We did not observe any holes further inside of the SAM. Therefore, the SAM primarily grows in a compact, isotropic form regardless of the model. All in all, the shape of the SAM looks similar for both models. μ_R (σ_R) values for the figure are 10.7 (0.7), 12.1 (0.8), 15.4 (0.74), and 17.3 (0.82) for the top left, top right, bottom left, and bottom right, respectively. Although both μ_R and σ_R of the pushing model are larger than those of the hopping model, the circularities of two models are quite similar. We found $N = 5.0$ (top left), 5.0 (top right), 5.8 (bottom left), and 5.9 (bottom right).

Instead of comparing SAMs at the same time as in Figure 3, we now examine the SAMs consisting of exactly the same number of molecules from both models. After dropping a total of 1000 molecules, we ran further simulations without molecular dropping until all the molecules eventually bound to the substrate. For three different dripping rates, $n^* = 0.1$, 1, and 10, we ran 10 independent simulations and averaged over the runs. In the case of a slowly dripping tip ($n^* = 0.1$), the average

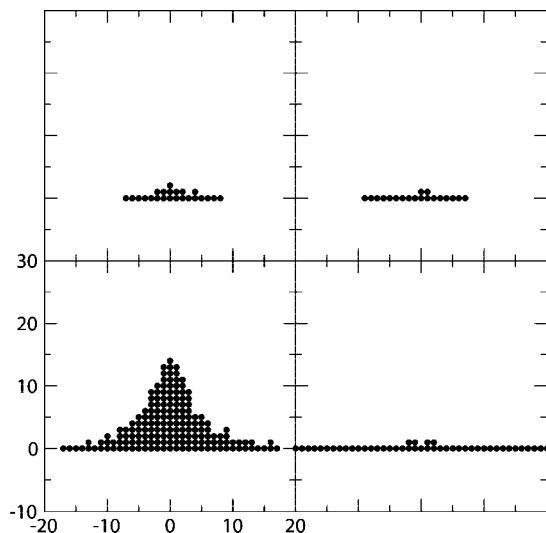


Figure 4. Side view of the droplet created under the tip. All snapshots are taken at $t = 250$. The dripping rate of the tip is $n^* = 1$ for the top two panels and $n^* = 10$ for the bottom two panels. For each n^* , the droplet from the hopping model (left panel) is compared to that of the pushing model (right panel).

circularity N is 6.2 (from $\mu_R = 17.4$ and $\sigma_R = 0.73$) and 5.7 (from $\mu_R = 17.4$ and $\sigma_R = 0.87$) for the hopping and the pushing models, respectively. For $n^* = 1$, N is 6.0 (from $\mu_R = 17.4$ and $\sigma_R = 0.78$) and 5.9 (from $\mu_R = 17.4$ and $\sigma_R = 0.82$) for the hopping and the pushing models, respectively. In the case of a fast dripping tip ($n^* = 10$), N is 6.0 ($\mu_R = 17.4$ and $\sigma_R = 0.78$) and 5.8 ($\mu_R = 17.3$ and $\sigma_R = 0.84$) for the hopping and the pushing models, respectively. Irrespective of n^* , the circularity of the pushing model is slightly less than that of the hopping model due to an increased σ_R . We additionally considered SAMs consisting of 100 or 10 000 molecules for both models. The SAMs from the pushing model are constantly lower in circularity. The lower circularity of the pushing model can be attributed to a relatively enhanced molecular mobility of the model.

Figure 4 shows a side view of a multilayered droplet below the tip (due to the molecular flux out of the tip). For the pushing and the hopping models, we show snapshots taken at $t = 250$ for $n^* = 1$ (top two panels) and 10 (bottom two panels). The droplet from the hopping model (top left and bottom left) is substantially taller and wider than that from the pushing model, especially for the fast dripping tip (bottom left). In the serial pushing model (top right and bottom right), the droplet is nothing more than several molecules sitting on top of the bottom monolayer. Due to the enhanced molecular mobility of the pushing model, the area below the tip is not as congested with molecules as in the hopping model. All the droplets in the figure look more or less symmetrical laterally. For the smallest dripping rate ($n^* = 0.1$, not shown), a multilayered droplet like in Figure 4 hardly exists for both models.

We now give a quantitative analysis of the radial growth of the SAM. We calculated the distance squared of each peripheral point from the center and averaged over all the peripheral points. In addition, we ran five independent simulation runs and averaged over the runs. Such an average of the distance squared is defined as the radius squared of the SAM, $R(t)^2$. Our simulation shows $R(t)^2$ from the pushing model is a linear function of time, showing a diffusive growth in its time dependence. In Figure 5, $R(t)$ is plotted as a function of time for various dripping rates, $n^* = 10$ (filled circles), 1 (filled diamonds), and 0.1 (filled triangles). For comparison, we plot $R(t)$ from the hopping model for each n^* (open symbols with

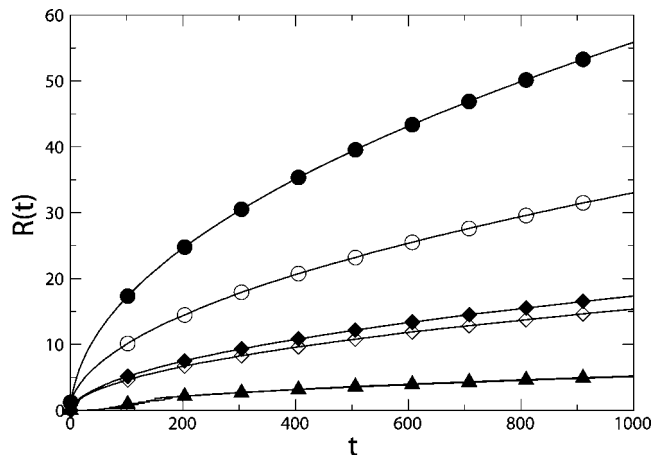


Figure 5. Time-dependent radius of self-assembled monolayer $R(t)$. $R(t)$ is plotted as a function of time t for dripping rates of $n^* = 0.1$ (filled triangles), 1 (filled diamonds), and 10 (filled circles). The data for each n^* look like a smooth curve because they are closely spaced. The symbols are drawn for every 100 time steps to distinguish different curves. For each n^* , $R(t)$ from the hopping down model is plotted for comparison (marked as open symbols with the same shape used for the pushing model).

the same shape as in the pushing model). In the continuous space limit, $R(t)^2$ in the hopping down model is analytically given by $R(t)^2 = \lambda^2 Dt$, where λ^2 is determined by the equation $\exp(-\lambda^2) = (4D\lambda^2)/(n/\pi)$.⁶ For a slowly dripping tip ($n^* = 0.1$), $R(t)$ values from the two models are indistinguishable. In the hopping down model, if the molecular dripping is extremely slow, molecules have plenty of time to self-assemble on the substrate between two consecutive dripping events. Then the molecular mobility D should not matter, and $R(t)$ depends on n only. An analytic expression $R(t)^2 = (n/\pi)t$ can be obtained in this limit.⁶ As the dripping rate increases to $n^* = 1$ and 10, however, the radial growth of the present model becomes faster than that of the hopping model. We fitted the radius squared from each model with a linear function of time, $R(t)^2 = at$, by using the least-squares method. As a measure of relative speed of radial growth, we calculated the ratio of a values from both models. The ratio was found to be 1.26 and 2.84 for $n^* = 1$ and 10, respectively. With an increase in the dripping rate, the radial growth from the pushing model becomes increasingly faster than that of the hopping down model.

Let us switch to the case of a moving tip. Now the tip scan speed enters as another variable in simulation. The top right and bottom right panels of Figure 6 sequentially show a line created by a tip moving upward with a speed of $v^* = 0.25$. The dripping rate n^* is 10, and the snapshots are taken at $t = 200$ (top right) and 500 (bottom right). Under the same conditions as above, a line created from the hopping model is drawn in the top left and bottom left. The line from the pushing model is fairly uniform in its width, but the line boundary of the hopping model looks like a parabola. Every line in the figure fluctuates in its periphery from a straight vertical line due to the nature of random walk. Although not shown here, for dripping rates smaller than 10, lines from two models become more similar than in the figure.

We consider more complex patterns generated by a moving tip. Using the same tip speed and dripping rate as in Figure 6, we have drawn in Figure 7 cross (top two panels) and gamma (bottom two panels) characters using the pushing and the hopping models. The crosses are generated by first drawing the vertical line (tip moving upward) and then the horizontal line

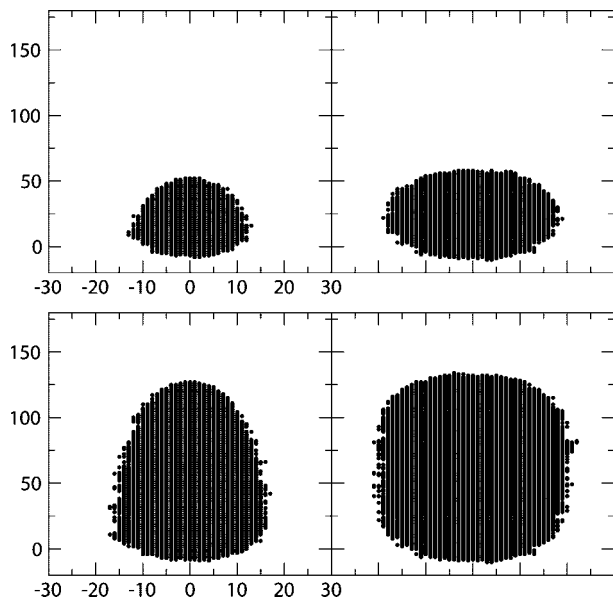


Figure 6. Line drawing by a moving tip. The tip is moving upward with a speed of $v^* = 0.25$, and its dripping rate is $n^* = 10$. The line from the serial pushing (hopping down) model is sequentially drawn in the top right and bottom right (top left and bottom left). The snapshots are taken at $t = 200$ (top two panels) and 500 (bottom two panels).

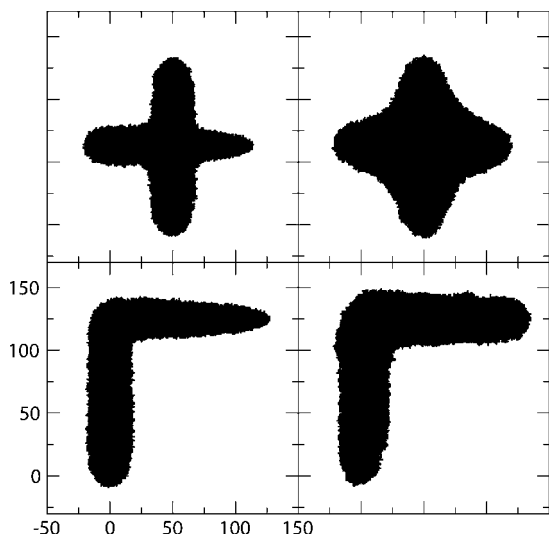


Figure 7. Cross and gamma characters drawn by a moving tip for the serial pushing (top right and bottom right) and hopping down (top left and bottom left) models. The tip scans with a speed of $v^* = 0.25$, and its dripping rate is $n^* = 10$. To create the cross, the tip moves vertically upward and then laterally from left to right. The gamma character is written similarly by first moving the tip upward and then laterally right. The snapshots are taken at $t = 1000$.

(tip moving left to right). At the crossing point, the pattern from the pushing model (top right) is substantially broadened due to the repeated dropping of molecules at the same spot. As already found in Figure 6, the pushing model (top right and bottom right) gives a line broader in width (both vertical and horizontal directions). Because of the large blurring at the center, the lines of the cross in the pushing model (top right) are not as uniform as in the hopping model (top left). The blurring of the SAM at the corner of the gamma character is also more significant in the pushing model (bottom right). Beside these details, the cross and gamma characters are qualitatively similar for both models.

The present serial pushing is directionally incoherent in that the molecular displacement induced by push takes a random

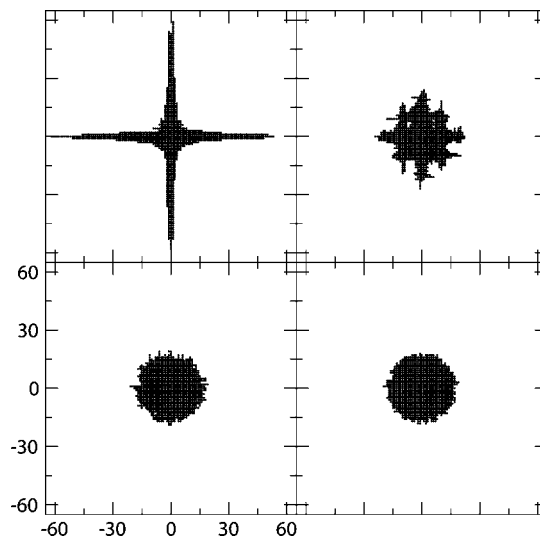


Figure 8. Self-assembled monolayers obtained by using various directional coherence lengths N_d . The tip is fixed, and $n^* = 1$. All the snapshots are taken at $t = 1000$. Shown in the top left is the monolayer where all the sequential pushes have the same direction as the initial pushing ($N_d = \infty$). In the top right and bottom left, we show the case where only a finite number of push-induced movements have the same direction. $N_d = 10$ (top right) and 5 (bottom left). For comparison, the default case of zero coherence length is shown in the bottom right.

direction. As discussed in the Details of Model and Simulation section, the directional coherence length N_d is zero in this case. We can choose a different N_d instead. If N_d is taken to be infinity, all the push-induced movements take the same direction as the initial pushing direction. The resulting SAM is a long, narrow cross except for the round broadening at the center (top left, Figure 8). The roundness of SAM at the center arises from the hopping down events which occasionally occur for a small sized SAM. The fourfold symmetry of branch structure arises from the anisotropy of the substrate (note there are only four lateral directions on the substrate). We also simulated the case where the directional coherence exists up to a finite number of consecutive movements. In the case of $N_d = 10$ (top right), the SAM is more compact than for $N_d = \infty$ and has many branches. As the thick branches near the center of the SAM extend outward, they ramify into smaller and shorter branches. One can still discern the fourfold symmetry arising from the substrate anisotropy. We also notice several holes in the SAM which are located somewhat inside (in contrast to the tiny hole very close to the periphery in Figure 3). A hole in this case develops from linking of branches during the SAM growth: the SAM starts out as a cross, and, as time goes by, the cross ramifies into a more complex structure. During the ramification, two growing branches join to give a hole like one of those shown in the top right of Figure 8. As N_d decreases to 5 (bottom left), the SAM becomes even more compact and its branches are shorter, less pronounced, and mainly located near the periphery. Now we do not see the fourfold symmetry of the SAM. The structure is quite analogous to the directionally incoherent case (shown for comparison in the bottom right), but it is more fluctuating in periphery and has longer branches.

It would be interesting to investigate how the above branch structure turns out for a substrate with different anisotropy. For example, Au (111) is a well-known substrate for DPN and has a trigonal lattice structure. Our preliminary simulation shows a sixfold hexagonal branch structure for the SAM in the case of a directionally coherent pushing. Here the substrate anisotropy plays out more interestingly. The two adjacent branches of a

growing hexagonal SAM sometimes join together to give a new branch growing in the middle direction of them. We also find the monolayer from the pushing model agrees well with that of the previous molecular dynamics simulation.¹⁰ A detailed account of the trigonal substrate will be presented elsewhere.

IV. Concluding Remarks

Motivated by the mechanism found in molecular dynamics simulations, we proposed a novel diffusion model for the dip-pen nanolithography. In this serial pushing model, molecules dropping from the tip push molecules on the substrate out of their original positions. If a molecule just pushed out jumps upon its own neighbor at still, another push is invoked. Such a sequential pushing propagates all the way from its origin to the periphery of the SAM. The consecutive push-induced movements occur instantaneously on the time scale of diffusion. By default, every push-induced move takes a random direction. This pushing model is in stark contrast with the previous hopping down model which forbids such a push due to the excluded volume effect. A molecule instead moves on top of immobile molecules trapped on the substrate. These seemingly disparate models give SAMs similar in shape. There is quantitative difference, however. Within the same amount of time, the SAM from the pushing model grows faster, and this difference becomes more significant as the tip dripping rate increases. When two SAMs of the same size are compared, the SAM from the pushing model deviates slightly more from a circle, probably due to the enhanced molecular mobility in the pushing model.

A salient feature of our model is the directional coherence length of push-induced displacement. This is the number of consecutive moves which take the same direction. Our default model opts for zero coherence length so that the direction of every displacement is random. The resulting SAM is compact and circular as in the hopping model. If we choose a finite value for the directional coherence length, however, a branched SAM forms. Depending on the value, the SAM has distinct branches extending far out from the center (for a large coherence length), or it becomes a compact dot with many short branches near its periphery (for a small coherence length). Due to the anisotropy of substrate (a square grid), the branched SAM shows a weak or pronounced fourfold symmetry. The versatility of the present model in generating various structures of a SAM (from a dot to a cross) represents an improvement over the previous hopping model which produces a compact circular SAM only. In some sense, the present model is inclusive of the hopping model. Note a hopping down is not prohibited in our model. In fact, for small SAMs, we occasionally observe hopping down events in simulation. As the SAM grows in size, however, a molecule on top is more likely to push out a molecule on the substrate rather than to step over molecules below and then hop down.

Instead of a sophisticated model of DPN, we here tried to come up with a simplistic model requiring a minimal set of parameters. A simple model will be easily adopted for interpretation of experiment and for implementation in computer programs. The previous hopping down model is limited in its scope of applicability because it assumes the extreme case of an irreversible trapping of a molecule by the substrate. The

present model, however, is grounded on the observations in molecular dynamics simulations. By systematically varying the parameters of the model (tip speed, dripping rate, and directional coherence length), we have demonstrated that diverse SAMs result. It is therefore reasonable to expect that the present model is applicable to a broader range of experimental systems compared to the hopping model. The obvious next step is to quantitatively compare our simulation with experiment. To do so, we need to obtain the appropriate values for the molecular diffusivity, the dripping rate, and the directional coherence length. This is not a trivial procedure, however. Especially, the exact determination of the diffusivity can be elusive because the diffusion in our model refers to a molecular motion on top of the SAM which is neither surface nor bulk diffusion. Leaving the connection to experiment as future work, the present work focused on investigating the key features of our model and on illustrating how the SAM is affected by various parameters of model.

Acknowledgment. This work was supported by the Korea Research Foundation Grant funded by the Korean Government (MOEHRD) Grant Nos. KRF-2005-070-C00065 and KRF-2008-521-C00123.

References and Notes

- (1) Salaita, K.; Wang, Y.; Mirkin, C. A. *Nat. Nanotechnol.* **2007**, *2*, 145.
- (2) Mirkin, C. A. *ACS Nano* **2007**, *1*, 79.
- (3) Ginger, D. S.; Zhang, H.; Mirkin, C. A. *Angew. Chem., Int. Ed. Engl.* **2004**, *43*, 30.
- (4) Moldovan, N.; Kim, K. H.; Espinosa, H. D. *J. Microelectromech. Syst.* **2006**, *15*, 204.
- (5) Kim, K. H.; Moldovan, N.; Espinosa, H. D. *Small* **2005**, *1*, 632.
- (6) Jang, J.; Hong, S.; Schatz, G. C.; Ratner, M. A. *J. Chem. Phys.* **2001**, *115*, 2721.
- (7) Jang, J.; Schatz, G. C.; Ratner, M. A. *Phys. Rev. Lett.* **2003**, *90*, 156104.
- (8) Lee, N. K.; Hong, S. *J. Chem. Phys.* **2006**, *124*, 114711.
- (9) Ahn, Y.; Hong, S.; Jang, J. *J. Phys. Chem. B* **2006**, *110*, 4270.
- (10) Heo, D. M.; Yang, M.; Hwang, S.; Jang, J. *J. Phys. Chem. C* **2008**, *112*, 8791.
- (11) Manandhar, P.; Jang, J.; Schatz, G. C.; Ratner, M. A.; Hong, S. *Phys. Rev. Lett.* **2003**, *90*, 115505.
- (12) Cho, N.; Ryu, S.; Kim, B.; Schatz, G. C.; Hong, S. *J. Chem. Phys.* **2006**, *124*, 024714.
- (13) Sheehan, P. E.; Whitman, L. J. *Phys. Rev. Lett.* **2002**, *88*, 156104.
- (14) Weeks, B. L.; Noy, A.; Miller, A. E.; De Yoreo, J. J. *Phys. Rev. Lett.* **2002**, *88*, 255505.
- (15) Peterson, E. J.; Weeks, B. L.; De Yoreo, J. J.; Schwartz, P. V. *J. Phys. Chem. B* **2004**, *108*, 15206.
- (16) Schwartz, P. V. *Langmuir* **2002**, *18*, 4041.
- (17) Salaita, K.; Amarnath, A.; Maspoeh, D.; Higgins, T. B.; Mirkin, C. A. *J. Am. Chem. Soc.* **2005**, *127*, 11283.
- (18) Hampton, J. R.; Dameron, A. A.; Weiss, P. S. *J. Phys. Chem. B* **2005**, *109*, 23118.
- (19) Rozhok, S.; Piner, R.; Mirkin, C. A. *J. Phys. Chem. B* **2003**, *107*, 751.
- (20) Rozhok, S.; Sun, P.; Piner, R.; Lieberman, M.; Mirkin, C. A. *J. Phys. Chem. B* **2004**, *108*, 7814.
- (21) Levi, A. C.; Kotrla, M. *J. Phys.: Condens. Matter.* **1997**, *9*, 299.
- (22) Boon, J. P.; Yip, S. *Molecular Hydrodynamics*; McGraw-Hill: New York, 1980.
- (23) Caudwell, D. R.; Trusler, J. P. M.; Vesovic, V.; Wakeham, W. A. *Int. J. Thermophys.* **2004**, *25*, 1339.
- (24) Haralick, R. M. *IEEE Trans. Syst. Man. Cybern.* **1974**, *4*, 394.